

# DEVELOPMENT OF A SOLID PROPELLANT GAS GENERATOR (SPGG) SYSTEM FOR FIRE SUPPRESSION IN AVIATION – DESIGN OF AN INJECTOR

Elizabeth Richter<sup>1</sup>, Ulrich Krause<sup>2</sup>

<sup>1</sup>Airbus Group Innovations, <sup>2</sup>Otto-Von-Guericke University Magdeburg

**Keywords:** *fire suppression, Solid propellant gas generator*

## Abstract

*The paper comprises the description a fire suppression system for the application in civil aircraft. Here the reason is the ban of current suppression medium which in 2018 extends to the aircraft sector [1] because this suppression system is based on the effective fire suppression medium Halon 1301 (Bromotrifluoromethane; CBrF<sub>3</sub>). At present various suppression alternatives are considered which pass the aircraft requirements and have the technical degree of maturity. An auspicious option tends to be Solid Propellant Gas Generator (SPGG). In this technique a propellant produces a scalding aerosol stream that is intended to suppress successfully an incipient fire via inhibition [2]. A challenge for this system is the scalding aerosol stream which is generated by chemical transformation of the propellant. To pass the aircraft requirements a cooling system is necessary. A feasible solution seems to be an injector that is normally used for rocket engines [3]. The theoretical calculation and the adaption of this are described in this paper. The design of the SPGG follows fluid dynamic guidelines of Abramowitsch [3] that are applied and verified by parameter verification using prototypes [4].*

## 1 Introduction

On board today's commercial aircraft fire suppression in inaccessible and normally not occupied areas, like the cargo holds, is realized by a system using a suppression agent called HALON 1301 (Bromotrifluoromethane; CBrF<sub>3</sub>). Since the European Commission decided to exclude the use of Halon for new aircraft type certificates after 2018 by the European Regulation (EC) No 1005/2009 aircraft manufacturer and airlines have been seeking for more than one decade for new fire suppression alternatives that are capable of fulfilling the aircraft requirements without compromising safety. A general requirement is that an alternative should be both – economically and ecologically reasonable. The system mass is directly connected with the fuel consumption that in turn leads to CO<sub>2</sub> and NO<sub>x</sub> emissions to the environment. Since the suppression system is rarely activated, the effect of preventing HALON release must not be surpassed by the effect of additional system mass. Therefore any new suppression system should be as lightweight as the current HALON based system in order to avoid other environmental impacts. One feasible option seems Solid Propellant Gas Generator technology which is further described in this paper.

### 1.1 SPGG general aims

SPGG system generates a suppression aerosol where the carrier medium is scalding aerosol gas and the dispersion media are salt particles. The main suppression function is realized by inhibition via salt particles while the inertization via scalding aerosol gas is a secondary extinguishing effect. But this scalding aerosol gas produces an impact of high temperature of more than 1200°C generated at transformation from a solid compound to the aerosol stream. Because of that fact a cooling system is necessary.

Commercial generators are available on the market; examples for this are products from companies like FirePro®, StatX®, Dynamenco®. These products are developed for ground based application, like protection of warehouses, server rooms, railway and other vehicles. They are commonly using solid material as ceramic structures for the cooling of the scalding aerosol stream. This cooling stack creates a considerable portion of the system weight, which is to be avoiding in aviation.

Alternatively the general idea of this approach is to create the cooling of the scalding aerosol stream via an injector as shown in Fig 1.

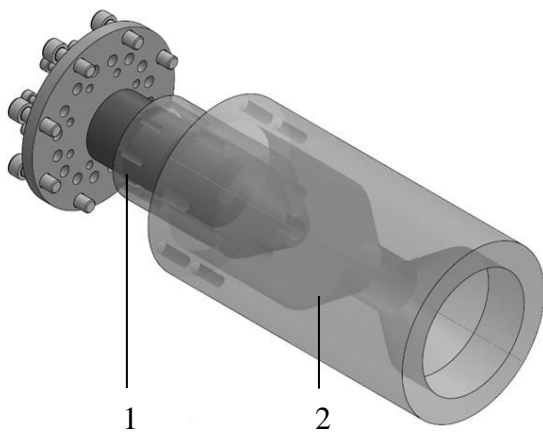


Fig. 1 SPGG with combustion chamber (1 – inside) and injector for cooling (2 – outside)

### 1.2 Combustion chamber of SPGG

The combustion chamber is that part of the generator where the solid compound is stored and where the aerosol stream is generated via a combustion process by transformation from

potassium nitrate, potassium nitrate and different carbon hydroxide compositions.

With the help of findings from the field of engine development a method is derived for the calculation of the SPGG combustion chamber [5]. Tests and simulations of the combustion chamber of SPGG in comparison with engine development are described in [4]. Here will adhere that the variation of the calculated temperature values of rocket motor and the tested values of combustion chamber of SPGG is in median 4%. Consequently the calculation of rocket motor achieves a high level of accuracy for the combustion chamber of SPGG and so it can be used for the SPGG calculation.

### 1.3 Cooling system of SPGG

For current SPGG application the cooling system is a built-in coolant which is in range of 30% of the system weight. To decrease the system weight it seems to be feasible to replace the cooling system via an injector. The work principle of the injector is mixing of the produced scalding aerosol gas from the combustion chamber with ambient air to realize the cooling. The design calculations of such an injector are the scope of this paper.

## 2 Determination of the SPGG injector

The determination of the injector has to consider parameters of the combustion chamber, the fluid flow at the mixing point after the nozzle, the mixing range and the component conditions of generator and injector.

The general equations for an injector design are described in various sources. Abramowitsch [3] has postulated a set of equations for the fundamental design of an injector. These equations have been applied and derived for the design in this paper. For the calculation it can be assumed that the particle inside the aerosol stream do not influence the gas flow because the particles are smaller than 50 micrometers [6].

## 2.1 Combustion chamber of SPGG

The combustion chamber contains the propellant and the determination includes the nozzle dimension. By dimensioning of the nozzle parameters like pressure, mass flux and velocity are defined. In eq. 1, the dimensionless quantity describing the ratio of speed of an object moving through a fluid and the local speed of sound is called Mach number of the combustion chamber ( $Ma_{cc}$ ), where  $v$  is the fluid velocity,  $\kappa$  is the adiabatic index,  $R$  is the specific gas constant and  $T$  is the temperature.

$$Ma_{cc} = \frac{v}{\sqrt{\kappa RT}} \quad (1)$$

The critical Mach number ( $Ma_0^*$ ) is another dimensionless quantity and can be described through the velocity ( $v$ ) and the critical velocity of sound ( $c^*$ ). It can be further described as in eq.2 by the Mach number in relation and the adiabatic index ( $\kappa$ ) which is the ratio of specific heat.

$$Ma_0^* = \frac{\frac{\kappa+1}{2} \cdot Ma^2}{1 + \frac{\kappa-1}{2} \cdot Ma^2} = \frac{v}{c^*} \quad (2)$$

In a theoretically perfect combustion the entire propellant is transformed to an aerosol stream. Parallel tests indicated that there is always a combustion residual, that impacted the aerosol mass flow and thereof its velocity. Therefore the critical velocity of sound is divided into the theoretical critical velocity ( $c_{(theo)}^*$ ) and an efficiency factor of the critical velocity ( $\eta_{c^*}$ ). Both are illustrated in eq. 3. The efficiency factor was estimated by the measurement of the compound and its residual after combustion.

Due to accuracy of the measurements at the nozzle the critical velocity of sound was estimated through gas constant ( $R$ ), molar mass ( $M$ ), critical temperature ( $T^*$ ) and adiabatic index ( $\kappa$ ).

$$c_{(eff)}^* = c_{(theo)}^* \cdot \eta_{c^*} = \frac{\sqrt{\frac{R}{M} \cdot T^*}}{\sqrt{\kappa} \cdot \left(\frac{2}{\kappa+1}\right)^{\frac{\kappa+1}{2 \cdot (\kappa-1)}}} \cdot \eta_{c^*} \quad (3)$$

The effective critical velocity of sound ( $c_{(eff)}^*$ ) together with the mass flux ( $\dot{m}$ ) and

critical pressure ( $p^*$ ) is used in Eq. 4 to determine the nozzle exit area ( $A^*$ ).

$$A^* = \frac{c_{(eff)}^* \cdot \dot{m}}{p^* \cdot 10^5} \quad (4)$$

Since for the prototype design the nozzle is designed by a circle area, the nozzle diameter ( $d^*$ ) can be deduced in Eq. 5 by the nozzle exit area ( $A^*$ ).

$$d^* = \sqrt{\frac{A^* \cdot 4}{\pi}} \quad (5)$$

Eq. 3, 4 and 5 describe the behavior of the mass flow in the combustion chamber and through the nozzle by fluid dynamics in which geometry data are determined by basic equations of rocket motor design. The determination of relevant parameter with respect to the processes in the combustion chamber of the SPGG and its verification are described in [4]. These are design data for these above described fluid dynamic functions.

## 2.2 Fluid stream of SPGG

The adequate description of the fluid stream is necessary for the design of the injector, for the construction and material selection of the generator and for the impact of the suppression agent to the aircraft system. This description shall be fulfilling the requirements.

Figure 2 shows the principle of injector. The fluid stream is indicated by relevant parameters (mass flux ( $\dot{m}$ ), pressure ( $p$ ), temperature  $T$ , velocity ( $v$ ) and area ( $A$ )) and different levels of the mass flow. Index 1 refers to the driving jet, index 2 represents the intake stream of the ambient air, index 3 considers the gas mixture of the driving jet with the intake gas mixing chamber and index 4 indicates the gas mixture at the outlet.

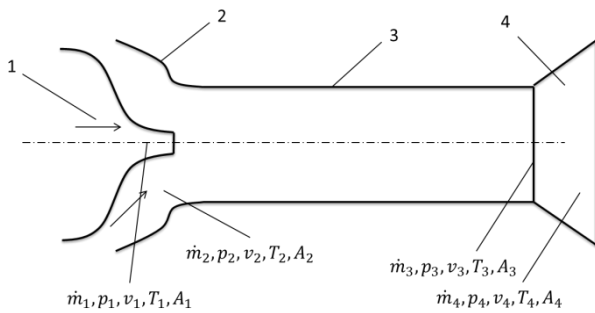


Fig. 2 Dimension of the whole system – combustion chamber (1), influent diffuser (2), injector (3), diffuser (4) – and there quantities according to [3].

In the injector, the total pressure of intake air is increased by the driving stream of higher pressure. The energy transfer of both streams is achieved by turbulent mixing. With increasing total pressure in the driving jet larger amounts of air can be drawn in. The injector is composed of a nozzle, an inlet of the intake gas, a mixing chamber and a diffuser. The position and shape of the nozzle and inlet have not much impact on the mixing process and the operating parameters of the injector. At cross section of the mixing chamber after the nozzle, a pressure is set which is smaller than the total pressure of the intake gas and the driving jet. However, both static pressures at this point become equal. The ratio of the two mass flows depends on the ratio of the nozzle cross section to the inlet cross section (Eq. 6) and condition of the mass flows. At the entrance of the mixing chamber the intake gas and the driving jet enter as two separate streams. They differ in their chemical composition, speed, temperature and total pressure. During the mixing of both streams their flow parameters compensate over the cross section. The driving stream contains particles of the intake gas and generates a negative pressure at the entrance of the mixing chamber, which causes the intake. The balance of both flows is then performed within the mixing chamber and results in a uniform gas mixture at the outlet. The larger the ratio of the mass flux of the

driving jet to that of the intake gas is the higher the total pressure of the gas mixture is at the outlet. The diffuser at the end of the mixing chamber then converts the kinetic energy to potential energy. The mixing process causes energy losses at the nozzle and the walls of the mixing chamber. This can be represented by the change of the kinetic energy. It is assumed that the mixing of the jets takes place at constant pressure. Then the product of mass flow and velocity is equal to the sum of the two gas streams. The losses of kinetic energy increase with the ratio of the speed of the driving jet to the inlet flow is. The balance of both streams in the mixing chamber leads to a decrease of the velocity of the mixture, and thus to an increase in the static pressure. The ratio of the cross sectional area of the nozzle to the cross-sectional area of the inlet is a major geometrical parameter  $\alpha$  (Eq. 6).

$$\alpha = \frac{A_1^*}{A_3} \quad (6)$$

The smaller  $\alpha$  is, the more gas can be sucked in while increasing only slightly the overall pressure. According to Abramowitch the mixing process need not to be considered for determination of the flow parameters at the outlet of the mixing chamber. Therefore the flow is only depending on the energy conservation law, the mass conservation law and the law of momentum.

Since the fluxes are considered to be equal these equations are sufficient to determine the parameters of the gas mixture at the outlet of the mixing chamber. From this the energy losses during mixing can be determined afterwards. Since the flows in the inlet cross-section of the mixing chamber are given, the flow variables, total temperature, Mach number, and the total pressure of the gas mixture can be determined in the outlet of the mixing chamber.

The mass conservation law can be depicted as Eq. 7.

$$\dot{m}_3 = \dot{m}_1 + \dot{m}_2 \quad (7)$$

Since there is a ratio between the mass flow of the driving jet and the inlet stream this can be expressed as Eq. 8.

$$n = \frac{\dot{m}_2}{\dot{m}_1} \text{ or } \dot{m}_2 = n \cdot \dot{m}_1 \quad (8)$$

Inserted into Eq. 7 leads to

$$\begin{aligned} \dot{m}_3 &= \dot{m}_1 + n \cdot \dot{m}_1 \text{ or} \\ \dot{m}_3 &= \dot{m}_1 \cdot (n + 1) \end{aligned} \quad (9)$$

Inserted into Eq. 7 leads to Eq. 9

$$\frac{\dot{m}_3}{\dot{m}_1} = n + 1 \quad (10)$$

When neglecting the heat transfer by the wall of the mixing chamber the energy conservation law leads to Eq. 11.

$$\dot{m}_3 \cdot c_{p3} \cdot T_3^* = \dot{m}_1 \cdot c_{p1} \cdot T_1^* + \dot{m}_2 \cdot c_{p2} \cdot T_2^* \quad (11)$$

Independently of the mixing process, the total enthalpy content in the mixed stream is equal of the sum of the enthalpy content of the single streams. Assuming that the specific heat of the gas streams ( $c_{p1} = c_{p2} = c_{p3}$ ) and dividing by the mass flows gives Eq.12.

$$\begin{aligned} \frac{\dot{m}_3}{\dot{m}_1} \cdot T_3^* &= \frac{\dot{m}_2}{\dot{m}_1} \cdot T_2^* + T_1^* \text{ or} \\ (n + 1) \cdot T_3^* &= n \cdot T_2^* + T_1^* \end{aligned} \quad (12)$$

Introducing the ratio between the temperatures of the driving jet and the inlet stream as  $\Theta$  in Eq.11

$$\Theta = \frac{T_2^*}{T_1^*} \quad (13)$$

The relation of the temperatures can be expressed as Eq.12 that enables to determine the stagnation temperature at the outlet of the mixing chamber.

$$\frac{T_3^*}{T_1^*} = \frac{n \cdot \Theta + 1}{n + 1} \quad (14)$$

With these ratios the calculation of the mixed temperature ( $T_3^*$ ) is feasible.

$$T_3^* = T_4^* = T_1^* \cdot \frac{n \cdot \Theta + 1}{n + 1} \quad (15)$$

The difference aims to control the pressure at the SPGG outlet without significant temperature impact and therefore the temperature after diffusor ( $T_4^*$ ) can be estimate as output temperature ( $T_3^*$ ). The permissible temperature is limited by global regulations like [7] to 75°C. The variable influence on the output temperature ( $T_3^*$ ) are mainly the ratio of the area ( $\alpha$ ), the combustion chamber temperature ( $T_1^*$ ) and the combustion chamber pressure ( $p_3^*$ ). The ratio of the area ( $\alpha$ ) influences the length of the injector ( $l_2$ ). The output temperature ( $T_3^*$ ), the output pressure ( $p_4^*$ ) and the length of the injector ( $l_2$ ) are therefore the important design factors for the system layout of SPGG in aircraft.

### 2.3 Geometry of the SPGG

Finally the preceding subchapter enables the calculation of the geometry of combustion chamber, injector and diffusor. Since the generator design is the first step for the calculation and the development of SPGG the generator geometry values are used as input information for the injector calculation. So with the following equations it is possible to generate an injector to keep the requirements.

#### Combustion chamber (1)

So it follows the values of the generator firstly the length of the nozzle ( $l_{\text{nozzle}}$ ) and the length of the combustion chamber.

$$l_{\text{nozzle}} = l_{\text{generator}} - l_{\text{cc}} \quad (16)$$

The nozzle diameter ( $d_1^*$ ) can be calculated with the next equation.

$$d_1^* = \sqrt{\frac{A_1^* \cdot 4}{\pi}} \quad (17)$$

If equation 13 convert to the area of the nozzle ( $A_1^*$ ) it results in equation 14.

$$A_1^* = \frac{\pi}{4} \cdot d_1^{*2} \quad (18)$$

The area of the combustion chamber ( $A_{\text{cc}}$ ) can be determined by the radius of the combustion chamber ( $R_{\text{cc}}$ ).

$$A_{\text{cc}} = \pi \cdot R_{\text{cc}}^2 \quad (19)$$

*Influent diffusor (2)*

The length of the influent diffusor ( $l_2$ ) are supposed to be equal to the nozzle length ( $l_{\text{Nozzle}}$ ).

$$l_2 = l_{\text{Nozzle}} \quad (20)$$

By this length the needed diameter of the influent diffusor ( $d_2$ ) and the arc of dwell ( $\beta_2$ ) can be calculated.

$$d_2 = d_1^* + 2 \cdot l_2 \cdot \tan\left(\frac{\pi}{180} \cdot \beta_2\right) \quad (21)$$

Through the influent diffusor diameter ( $d_2$ ) the area of the influent ( $A_2$ ) can be detected.

$$A_2 = \frac{\pi}{4} \cdot d_2^2 \quad (22)$$

*Injector (3)*

With the area of the nozzle ( $A_1^*$ ) and the area ratio ( $\alpha$ ) can be determined the diameter of the injector ( $d_2$ ).

$$d_2 = d_3 = \left( 4 \cdot A_1^* \cdot \left( \frac{1 + \frac{1}{\alpha}}{\pi} \right) \right)^{0,5} \quad (23)$$

The length of the injector ( $l_3$ ) is dependent of the diameter of the injector ( $d_3$ ) and a factor ( $l_3/d_3$ ) which is described in [3] as value between six and ten. The optimal injector length will be determined by testing. But it is also possible to calculate this value theoretically.

$$l_3 = \frac{l_3}{d_3} \cdot d_3 \quad (24)$$

Furthermore it is possible to calculate the outflow area of the injector ( $A_3$ ).

$$A_3 = \frac{\pi}{4} \cdot d_3^2 \quad (25)$$

*Diffusor (4)*

The length of the diffusor ( $l_4$ ) is dependent on the injector length ( $l_3$ ) and the ratio of diffusor and injector length ( $l_4/l_3$ ).

$$l_4 = l_3 \cdot \frac{l_4}{l_3} \quad (26)$$

So the diameter of the diffusor ( $d_4$ ) and with that the area of diffusor ( $A_4$ ) can be calculated. Here is  $\beta_4$  the arc of the diffusor outflow.

$$d_4 = d_3 + 2 \cdot l_4 \cdot \tan\left(\frac{\pi}{180} \cdot \alpha\right) \quad (27)$$

$$A_4 = \frac{\pi}{4} \cdot d_4^2 \quad (28)$$

The system of equations enables the theoretical calculation of the optimal injector. Dependent on the assembly area so the place inside the aircraft for installation there are more than one option for the dimension of such SPGG. The area ratio ( $\alpha$ ), the combustion chamber pressure ( $p_1^*$ ) and the combustion chamber temperature ( $T_1^*$ ) are values which will be determined by testing.

**3 Experimental Validation of the analytic method by setting up a corresponding injector**

The target of the chapter is the description of the test set-up and the discussion of the efficiency of the formulation in comparison with the fluid dynamic calculations.

**3.1 Test of the corresponding injector**

The calculation of injector in last chapter is applied to generate a prototype of SPGG with a temperature output of 348 K[7] as design criteria. The input-data for the values inside the combustion chamber deviate from a first test series [4]. Then the values for an injector are calculated. For this test of the injector is used a simplified design which only include the injector tube as illustrated in Fig. 3.

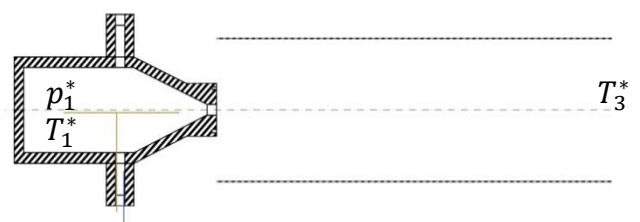


Fig. 3 Draft of simplified design for the test with combustion chamber (left) and injector (right)

This design is tested with 200, 400 and 600 gram propellant at constant nozzle dimension because different pressure values ( $p_1^*$ ) are needed to analyze the influence of the output temperature ( $T_3^*$ ). Therefore temperature sensors are positioned inside the combustion chamber, inside the nozzle and inside the outflow of the injector.

### 3.2 Results of the test

The analyses of the test values occur on the temperature in the outflow ( $T_3^*$ ). The various charges affect to pressure inside the combustion chamber of 3, 6 and 15 bar in order to the propellant mass. In table 2 the output temperature for the various pressure values.

Table 1 Test results of the injector test

Combustion chamber pressure ( $p_1^*$ ) in bar	Measured outflow temperature ( $T_3^*$ ) in K	Required outflow temperature ( $T_3^*$ ) in K
2.79	375	348
5.76	499	
14.84	581	

The difference between the calculated and the measured temperature values is 27 up to 233 K, at which the difference increase by higher pressure. All other input values are constant. Reason for the wide variation can be derived from imprecise input-values and this influence of the output temperature.

### 4 Summary

The theoretical adaption of an injector as cooling system for SPGG is feasible but it does not fulfil the temperature requirements of 75°C [7]. The testing of such SPGG results in a higher output temperature as required. The cooling from temperatures between 1200 °C and 1500 °C down to 348 K is the target of aircraft agency (for example European Aviation Safety Agency – EASA). The test of a first calculated injector with pressure of 3, 5, and 15 bar shows variations of the tested and calculated temperature value from 27 to 233 K. The challenge for further investigation is the optimization the geometry of an injector relating to the design of influent diffusor, area ratio of nozzle and injector diameter ( $\alpha$ ) and the combustion chamber values ( $T_1^*$ ,  $p_1^*$ ). So it enables a higher level of accuracy for the calculation methods of the injector and the future application of SPGG.

However a strong influence of the temperature output ( $T_3^*$ ) is determined by input

values which is summarized in the following table. Here is  $T_1^*$  the temperature in the combustion chamber,  $T_2^*$  the temperature of ambient air,  $p_1^*$  the pressure in the combustion chamber,  $p_2^*$  the pressure of the ambient air and  $\alpha$  the area ratio of nozzle and injector. Target for the next step is to decrease the output temperature ( $T_3^*$ ) to 348 K. An implementation of such temperature decrease is summarized in tab. 2 and can be realized by reduction of the temperature in combustion chamber ( $T_1^*$ ), the temperature of ambient air ( $T_2^*$ ), the pressure in combustion chamber ( $p_1^*$ ) or the area ratio of nozzle and inlet ( $\alpha$ ). In opposite to the temperature value which have a direct impact the pressure and the area ratio affect the mass flux in direction of an effective gas mixture. The mass flux can be also balanced with an increase of the ambient pressure ( $p_2^*$ ).

Table 2 Summarized influence of output temperature via input data

Input	Required output
$T_1^* \downarrow$	
$T_2^* \downarrow$	
$p_1^* \downarrow$	$T_3^* \downarrow$
$p_2^* \uparrow$	
$\alpha \downarrow$	

These influences can be illustrated via the combination of eq. 15 and insertion of eq. 6 and 8.

$$T_3^* = T_1^* \cdot \frac{\frac{\dot{m}_2}{\dot{m}_1} \cdot \frac{T_2^*}{T_1^*} + 1}{\frac{\dot{m}_2}{\dot{m}_1} + 1} \quad (29)$$

An adjustment of these values especially temperature ( $T_1^*$ ) and pressure ( $p_1^*$ ) in the combustion chamber needs to prove in further test campaign.

It is recommended that a next test campaign shall be started with an injector using constant values for the pressure in the combustion chamber to prove the concept of SPGG relating to the aircraft requirements.

**List of symbols**

$A_1^*$	Area of the nozzle
$A_2$	Area of the influent
$A_3$	Area of the injector
$A_4$	Area of diffuser
$A_{cc}$	Area of the combustion chamber
$A^*$	Critical Area
$c_{p1}$	Specific heat of the combustion stream
$c_{p2}$	Specific heat of the sucked air
$c_{p3}$	Specific heat of the mixed airstream
$c_{(eff)}^*$	effective critical velocity of sound
$c_{(theo)}^*$	theoretical critical velocity
$c^*$	Critical velocity
$d_1$	nozzle diameter
$d_2$	Influent diffuser diameter
$d_3$	Injector diameter
$d_4$	Diffuser diameter
$l_2$	length of the influent diffuser
$l_3$	length of the injector
$l_4$	length of the diffuser
$l_3/d_3$	Factor [3]
$l_4/l_3$	ratio of diffuser and injector length
$l_{cc}$	Length of combustion chamber
$l_{generator}$	Length of generator
$l_{Nozzle}$	Length of nozzle
$M$	Molar mass
$Ma$	Mach number
$Ma_0^*$	Critical Mach number
$Ma_{cc}$	Mach number of the combustion chamber
$\dot{m}$	Mass flux
$\dot{m}_1$	Mass flux combustion chamber gas
$\dot{m}_2$	Mass flux sucked ambient air
$\dot{m}_3$	Mass flux mixing gas
$n$	Ratio of mass flux
$p^*$	Critical pressure
$p_1^*$	Critical pressure combustion chamber
$p_2^*$	Critical pressure sucked stream
$p_3^*$	Critical pressure mixed stream
$R$	gas constant
$R_{cc}$	Combustion chamber radius
$T_1^*$	Critical temperature combustion chamber
$T_2^*$	Critical temperature sucked stream
$T_3^*$	Critical temperature mixed stream

$v$	Velocity
$\alpha$	Area ratio
$\beta_2$	Arc of influent diffuser
$\beta_4$	Arc of outflow diffuser
$\kappa$	adiabatic index
$\eta_{c^*}$	efficiency factor of the critical velocity
$\pi$	Pi

**References**

- [1] United States Environment Program *Montreal Protocol on Substances that Deplete the Ozone Layer*. Montreal, 1987
- [2] Rempe A. *Praxishandbuch für den betrieblichen Brandschutz*. Kessler Verlagsdruckerei, 2004
- [3] Abramowitsch G. N. *Angewandte Gasdynamik*. VEB Verlag Technik Berlin, 1958
- [4] Richter E. and Krause U. Development of a solid propellant gas generator (SPGG) system for generating aerosols for fire extinguishing in aviation – Calculation and Testing of combustion chamber. *Fire in Vehicles*, Berlin, Vol. 3, paper number, pp 185-190, 2014.
- [5] Kubota N. *Propellants and Explosives – Thermochemical Aspects of Combustion*. Wiley-VCH Verlag GmbH, 2002
- [6] Böttner C.-U. *Über den Einfluss der elektrostatischen Feldkraft auf turbulente Zweiphasenströmungen*. Online Ressource: <http://sundoc.bibliothek.uni-halle.de/diss-online/02/03H036/prom.pdf>, 2002
- [7] *Fixed firefighting systems – Condensed aerosol extinguishing systems – Part 1: Requirements and test methods for components*. German version CEN/TR 15276-1:2009

**Contact Author Email Address**

elizabeth.richter@eads.net

**Copyright Statement**

The authors confirm that they, and/or their company or organization, hold copyright on all of the original material included in this paper. The authors also confirm that they have obtained permission, from the copyright holder of any third party material included in this paper, to publish it as part of their paper. The authors confirm that they give permission, or have obtained permission from the copyright holder of this paper, for the publication and distribution of this paper as part of the ICAS 2014 proceedings or as individual off-prints from the proceedings.